New field-induced single ion magnets based on prolate Er(III) and Yb(III) ions: tuning the energy barrier U_{eff} by the choice of counterions within N_3-tridentate Schiff-base scaffold

Supplementary Information

Adam Gorczyński,*[a#] Dawid Marcinkowski,[a#] Maciej Kubicki,[a] Marta Löffler,[b] Maria Korabik*,[b] Mirosław Karbowiak,[b] Piotr Wiśniewski,[c] Czesław Rudowicz,[a,1] and Violetta Patroniak*[a]

[a.] *Faculty of Chemistry, Adam Mickiewicz University, Umultowska 89b, 61614 Poznań, Poland; E-mail: adam.gorczynski@amu.edu.pl; violapat@amu.edu.pl;*
[b.] *Faculty of Chemistry, University of Wrocław, 14 F. Joliot-Curie, 50-383 Wrocław, Email: maria.korabik@chem.uni.wroc.pl;*
[c.] *Institute of Low Temperature and Structure Research, Polish Academy of Sciences, 2 Okolna,50-422 Wrocław*
[#] *Equal contribution of the two authors*
[1] *Visiting Professor; On leave of absence from: Institute of Physics, West Pomeranian University of Technology Szczecin, Al. Piastów 17, 70-310 Szczecin, Poland*

Table of contents

Table S1 Selected geometrical parameters with standard uncertainties (s.u.'s) in parentheses of [Er**L**$_2$(OTf)(MeOH)$_2$](OTf)$_2$ (**1**), [Yb**L**$_2$(OTf)$_2$](OTf) (**2**) complexes. For clarity the hydrogen atoms are not listed. The shortest coordination bonds are highlighted in red colour.

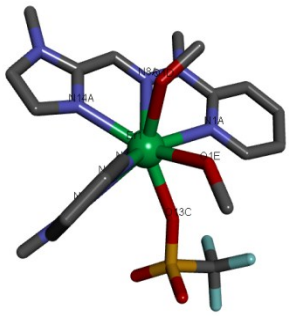

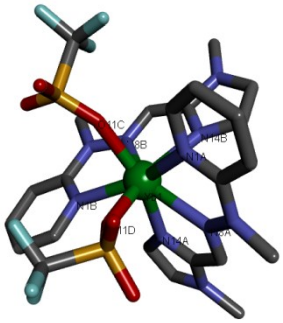

1 Er-OTf			**2 Yb-OTf**	
Bond	**Distance [Å]**		**Bond**	**Distance [Å]**
M-N1A	2.521(7)		M-N1A	2.475(6)
M-N8A	2.572(6)		M-N8A	2.480(6)
M-N14A	2.464(6)		M-N14A	2.390(7)
M-N1B	2.514(6)		M-N1B	2.470(6)
M-N8B	2.557(6)		M-N8B	2.512(6)
M-N14B	2.446(6)		M-N14B	2.402(7)
M-O13C	**2.332(5)**		**M-O11C**	**2.255(5)**
M-O1D	**2.391(5)**		**M-O11D**	**2.235(6)**
M-O1E	2.435(6)		---	---
Dihedral angle [°]			**Dihedral angle [°]**	
N1A-C2A-C10A-N14A	-1.41		N1A-C6A-C10A-N14A	-7.16
N1B-C2B-C10B-N14B	-0.13		N1B-C6B-C10B-N14B	9.36
Minimal distance between Er(III) centers: 9.47 Å			**Minimal distance between Yb(III) centers:** 9.80 Å	

Table S2 SHAPE analysis for lanthanide complexes, which assumes coordination number 9 for Ln(III) central metal ion. The lowest values of CShM are highlighted in red colour.

Shape	Symmetry	Er-OTf-(1)	Er-NO_3-(3)	Yb-NO_3-(4)
Enneagon	D_{9h}	34.290	33.626	33.266
Octagonal pyramid	C_{8v}	22.879	22.421	21.523
Heptagonal bipyramid	D_{7h}	18.633	17.618	16.188
Capped cube (Elongated square pyramid, J8)	C_{4v}	10.028	10.130	9.554
Capped cube		8.943	9.063	8.402
Capped sq. antiprism (Gyroelongated square pyramid J10)		1.896	2.464	2.549
Capped square antiprism		1.129	**1.586**	**1.718**
Tricapped trigonal prism (J51)	D_{3h}	1.750	3.016	2.844
Tricapped trigonal prism		**0.971**	2.329	2.146
Trivacant cuboctahedron	C_{3v}	14.267	13.592	13.083
Tridiminished icosahedron (J63)		12.380	11.441	11.880
Hula-hoop	C_{2v}	11.006	10.290	10.348
Muffin	C_s	1.700	1.841	2.124

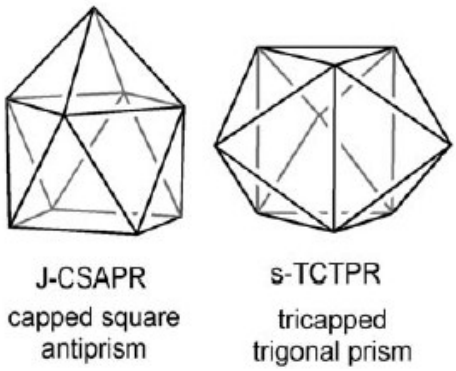

Table S3 SHAPE analysis for lanthanide complexes, which assumes coordination number 8 for Yb(III) central metal ion. The lowest values of CShM are highlighted in red colour.

Shape	Symmetry	Yb-OTf-(2)
Octagon	D_{8h}	30.704
Heptagonal pyramid	C_{7v}	24.239
Hexagonal bipyramid	D_{6h}	13.319
Cube	O_h	10.787
Square antiprism	D_{4d}	2.913
Elongated trigonal bipyramid	D_{3h}	22.819
Johnson - Elongated triangular bipyramid (J14)		25.685
Triangular dodecahedron (DD)	D_{2d}	**1.845**
Snub disphenoid (J84)		2.347
Johnson - Gyrobifastigium (J26)		10.331
Johnson - Biaugmented trigonal prism	C_{2v}	2.662
Biaugmented trigonal prism		2.430
Triakis tetrahedron	T_d	11.549

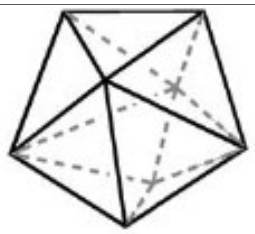

DD

Table S4 CSD search of Er(III) complexes (per analogy to **1**) that adopt ErN_6O_3 coordination sphere.

Entry	CSD Refcode	Additional information (FAC and MER refers to O_3)	Magnetic properties	References
1	BELHAC	Heterobimetallic helicate; – FAC coordination	---	[2]
2	FUNFAC	Homobimetallic helicate – FAC coordination	**Field induced SMM** U_{eff}/k_B = 9.5 K $\tau_0 = 1.08 \times 10^{-6}$ s (Orbach)	[3]
3	HUHMOM	Monometallic – MER coordination	---	[4]
4	ISAZIL	Monometallic – MER coordination	---	[5]
5	ITOCUR	Monometallic – MER coordination. **High degree of similarity!**	**Field induced SIM** U_{eff}/k_B = 30.4 K $\tau_0 = 7.8 \times 10^{-8}$ s (Orbach) U_{eff}/k_B = 49.2 K $\tau_0 = 3.8 \times 10^{-9}$ s (Raman+Orbach)	[6]
6	ITODIG		**Field induced SIM** U_{eff}/k_B = 25.8 K $\tau_0 = 3.5 \times 10^{-8}$ s (Orbach)	
7	PEBRIY	Monometallic – FAC coordination	Only effective magnetic moments	[7]
8	RIVPUJ	Monometallic – MER coordination	---	[8]
9	TUMJEQ	Monometallic – MER coordination	---	[9]
10	XENRAL	Monometallic – FAC coordination	---	[10]

Table S5 CSD search of Yb(III) complexes (per analogy to **2**) that adopt YbN_6O_2 coordination sphere.

Entry	CSD Refcode	Additional info	Magnetic properties	References
1	CAYRAX	Monometallic	---	11
2	DIMJAM	Homobimetallic	---	12
3	FUNDUP	Homobimetallic	DC and AC studies done; no SMM properties	3
4	GIFDAA (and GIFDAA10)	Monometallic	---	13, 14
5	HIRWUA	Heterobimetallic – YbCr	Only the variable temperature magnetic susceptibilities; χmT – 4.45 $cm^3 \cdot mol^{-1} \cdot K$ (max) to 3.8 $cm^3 \cdot mol^{-1} \cdot K$ at 4K Quote: [15]"quantitative analysis of the Yb complexes must await further detailed examination for the magnetic behavior"	15
6	IJOCIV	Monometallic	---	16
7	KAZTUA (and KAZTUA10)	Monometallic	---	17, 18
8	KEJWIF (and KEJWIF10)	Monometallic	---	
9	KOJLAX	Monometallic	---	19
10	KOJLEB			
11	MUVGAN	Monometallic	---	20
12	NOMGUS	Heterotetrametallic – Yb_2Li_2	---	21
13	NULXUN	Homobimetallic	---	22
14	OBIBEH	Homobimetallic	---	23
15	POJWEQ	Monometallic	---	24
16	POLGED	Monometallic	---	25
17	PULNEP	Heterotrimetallic – YbNiYb	---	26
18	QARBUH	Monometallic High degree of similarity!	---	27
19	QIVBUS	Heterobimetallic – YbCr	---	28
20	QIVCAZ	Monometallic	---	
21	TACJUE	Monometallic	---	29
22	TUDBEA	Monometallic	---	30
23	TUDBIE	Monometallic	---	
24	WAHFIX	Heterotrimetallic – $YbMo_2$	DC and AC studies done; no SMM behavior	31
25	WAHCUG			
26	YIPJOX	Monometallic	---	32

Table S6 Selected geometrical parameters with s.u.'s in parentheses of [Er**L**$(NO_3)_3(H_2O)$] (**3**). For clarity the hydrogen atoms are not listed. For clarity the hydrogen atoms are not listed. The shortest coordination bonds are highlighted in red colour.

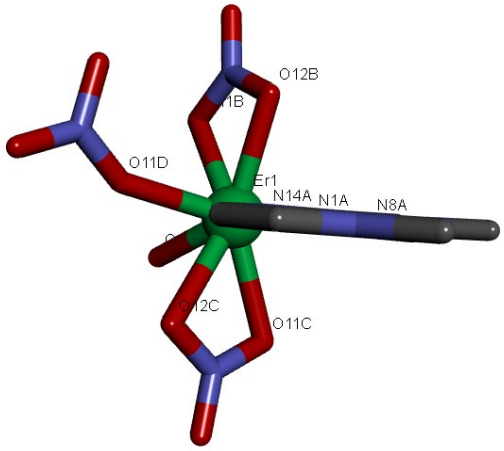

3 Er – NO_3		
Bond	**Location**	**Distance [Å]**
M-N1A	Basal plane ligand	2.446(8)
M-N8A		2.506(9)
M-N14A		2.409(9)
M-O1E	Basal plane solvent – H_2O	**2.357(7)**
M-O11D	Basal plane monodentate nitrate	**2.302(7)**
M-O11B	Bidentate nitrate – below basal plane	2.460(7)
M-O12B		2.381(7)
M-O11C	Bidentate nitrate – above basal plane	2.426(7)
M-O12C (apical anion)		2.436(7)
Dihedral angle of N1A-C6A-C10A-N14A: 1.55 °		
Minimal distance between Er(III) centers: 5.86 Å		

Table S7 Selected geometrical parameters with s.u.'s in parentheses of [Yb**L**$(NO_3)_3$(MeOH)]·MeCN (**4**). For clarity the hydrogen atoms are not listed. For clarity the hydrogen atoms are not listed. The shortest coordination bonds are highlighted in red colour.

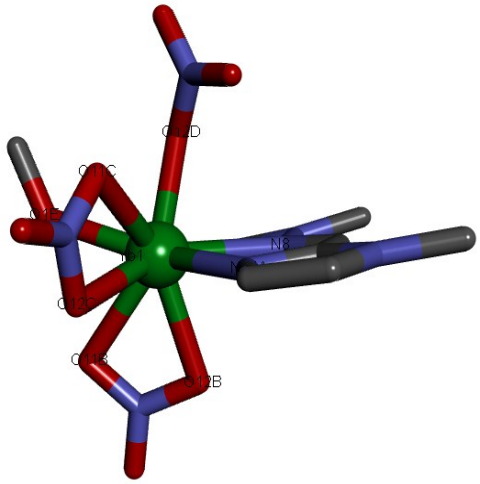

4 Yb – NO_3		
Bond	**Location**	**Distance [Å]**
M-N1A	Basal plane ligand	2.461(6)
M-N8A		2.486(7)
M-N14A		2.419(6)
M-O1E	Basal plane solvent – MeOH	2.331(5)
M-O12D	Monodentate nitrate – above basal plane	**2.251(5)**
M-O12C	Bidentate nitrate – basal plane	2.381(5)
M-O11C	Bidentate nitrate – above basal plane	2.451(5)
M-O11B	Bidentate nitrate – below basal plane	2.440(6)
M-O12B		2.402(5)
Dihedral angle of N1A-C6A-C10A-N14A: 0.65 °		
Minimal distance between Yb(III) centers: 5.95 Å		

Table S8 CSD search of Er(III) complexes (per analogy to **3**) that adopt ErN_3O_6 coordination sphere.

Entry	CSD Refcode	Additional information (FAC and MER refers to N_3)	Magnetic properties	References
1	AQAHIJ	Homobimetallic – MER coordination	---	33
2	BAGBER	Monometallic – MER coordination; 2 bidentate axial nitrates, equatorial acetylacetonate	---	34
3	BUZDEG	Bimetallic – MER coordination	---	35
4	CAQGEG	Monometallic – MER coordination; 2 bidentate axial nitrates, one bidentate equatorial nitrate	---	36
5	CIGYIC	Monometallic – MER coordination; one bidentate axial nitrate, two water molecules	---	37
6	COKPEY	Heterotetrametallic $ErAg_3$ – MER coordination	---	38
7	DUCQUN	Monometallic – MER coordination; two bidentate axial nitrates, two equatorial water molecules	---	39
8	DULMON	Monometallic – MER coordination; two bidentate axial nitrates, equatorial acetylacetonate	---	40
9	DUVPAM	Monometallic – MER coordination	---	41
10	FAZQEC	Monometallic – MER coordination; two bidentate axial nitrates, monodentate equatorial nitrate, equatorial MeOH; Isostructural to **21**	---	42
11	FUDKUL	Monometallic – MER coordination	---	43
12	GAMRAP	Homobimetallic – MER coordination	---	44
13	GESGER	Homobimetallic – MER coordination	---	
14	ILUGIG	Heterotrimetallic polymer – $ErCo_2$; MER coordination	Only DC measurements; The magnetic coupling interactions between d-and f-metal ions in the series of [Fe–L1–Ln], [Co–L1–Ln] and [CoII–L2–Ln] coordination polymers were explicitly characterized.	45
15	ILUGOM	Heteropentametallic polimer – Er_2Fe_3;		
16	JAGJAD	Monometallic – MER coordination; two bidentate axial nitrates, two equatorial water molecules	---	46
17	JUZVIL	Homobimetallic – FAC and MER coordination	DC measurements; Only for Dy very weak AC signal was observed	47
18	KEPZIP	Monometallic – MER coordination	---	48
19	KIBJOV	Monometallic – MER coordination;	---	49
20	KUNTAP	Monometallic – MER coordination; one bidentate axial nitrate, one axial and one equatorial water molecule, one equatorial and one axial DMF molecules	---	50
21	LAHPEQ	Heterotetrametallic – $ErNa_3$; MER coordination	---	51
22	LAHPEQ01		---	52
23	LUWXIL	Monometallic (Co-Er ionic salt) – MER coordination	---	53

24	NALCEJ	Monometallic (Co-Er ionic salt) – MER coordination	---	54
25	OCIVED	Heterobimetallic coordination polymer – ErCo; MER coordination	Weak antiferromagnetic exchange coupling interactions	55
26	ODELAM	Heterobimetallic coordination polymer – ErMn; MER coordination		
27	PERFOI	Homobimetallic; MER coordination	---	56
28	QIBRUP	Homobimetallic helicate; MER coordination	---	57
29	TEHDER	Homobimetallic helicate; MER coordination	---	58
30	TUGYEA	Heterotrimetallic; ErK_2; Mer coordination	---	59
31	TUVDUJ	Heteropentametallic polymeric assembly: Er_2Mn_3 – MER coordination	---	60
32	UGUHEK	Homotetrametallic polymeric assembly – MER coordination	---	61
33	UMIWOE	Homobimetallic – MER coordination	---	62
34	UQONAQ	Homobimetallic – MER coordination	---	63
35	VAJNIF	Heterooctametallic coordination polymers: Er_2Cu_6 –MER coordination	---	64
36	VUKNOG	Monometallic – MER coordination; 2 bidentate axial nitrates, equatorial DMSO	Erbium analogue was not studied for SIM behavior; Dy congener displayed SIM properties	65
37	WOPFAJ i	Heteropentametallic coordination polymers; Er_2Mn_3 – MER coordination;	DC measurements; Ferromagnetic interactions	66
38	WOPFIR	Heteropentametallic coordination polymers; Er_2Zn_3 – MER coordination;		
39	XECQIF	Monometallic – MER coordination	---	67
40	XEJBOF	Heterotetrametallic coordination polymer; ErK_3 – MER coordination	---	68
41	XIDTAG	Heterotetrametallic coordination polymer; Er_2K_2 – MER coordination	---	69
42	XITYEG	Monometallic – MER coordination; ; two bidentate axial carboxylates, one equatorial monodentate carboxylate, one equatorial water molecule	---	70
43	YAZXOO	Heterotetrametallic – Er_2Mn_2 – FAC coordination	Antiferromagnetic interactions; SMM behaviour was investigated - AC below 6 K but without any observed maxima	71
44	YUMGOC	Monometallic (Cr-Er ionic salt) – FAC coordination	---	72
45	ZOPNUP	Heterobimetallic coordination polymers ErSr – MER coordination	---	73

Table S9 CSD search of Yb(III) complexes (per analogy to **4**) that adopt YbN_3O_6 coordination sphere.

Entry	CSD Refcode	Additional information (FAC and MER refers to N_3)	Magnetic properties	References
1	AQAHEF	Homobimetallic – MER coordination	---	33
2	ARUQEJ	Monometallic – MER coordination; two bidentate axial nitrates, one equatorial bidentate nitrate	---	74
3	ASUHIF	Monometallic – MER coordination	---	75
4	CAQGAC	Monometallic – MER coordination; two bidentate axial nitrates, one equatorial bidentate nitrate	---	36
5	CAYZOT	Homotetrametallic – MER coordination	---	76
6	COVCEW	Heterotrimetallic – Yb_2K: MER coordination	---	77
7	DUCSEZ	Monometallic – MER coordination; two bidentate axial nitrates, two equatorial water molecules;	---	39
8	DUCTOK	Monometallic – MER coordination; two bidentate axial nitrates, monodentate equatorial nitrate, equatorial water; Similar to **23**	---	
9	DUXXOL	Monometallic – MER coordination; three acetylacetonates (2 ax. 1 eq.)	Yb(III) analogue was probed for SIM behavior but without observation of slow relaxation of magnetisation; Isostructural Dy analogue was found to display slow relaxation of magnetization	78
10	EFIZIC	Monometallic – MER coordination; two bidentate axial nitrates, monodentate equatorial nitrate, equatorial EtOH; Similar to **23**	---	79
11	EFIZUO	Monometallic – MER coordination; two bidentate axial nitrates, two equatorial water molecules;	---	
12	EVEGAN i	Heteropentametallic coordination network – Yb_2Mn_3	---	80
13	EVEGER	Heterodecametallic coordination network – Yb_4Mn_6	---	
14	FEWQEE	Monometallic – MER coordination; two bidentate axial nitrates, one equatorial bidentate nitrate	---	81
15	FONQUU i FONQUU01	Monometallic – MER coordination; 2 bidentate axial nitrates, equatorial acetylacetonate	---	34, 82
16	FONTEH	Monometallic – MER coordination; one bidentate axial nitrate, one axial acetylacetonate, one equatorial acetylacetonate	---	82
17	GEXHAU	Monometallic – MER coordination	---	83
18	HABMIH i HABMIH01	Homobimetallic – FAC coordination	---	84
19	HAWQUT	Monometallic – MER coordination	---	85
20	HAWRAA	Monometallic – MER coordination	---	

21	HIMFIT	Heterotrimetallic Yb_2Pt – MER coordination; three acac molecules	---	
22	HOYTIZ	Heterotetrametallic coordination network – $YbCs_3$; MER coordination	---	86
23	IJOCER	Monometallic – MER coordination; two bidentate axial nitrates, equatorial DMSO	---	16
24	ILUGAY	Heterotrimetallic polymer – $YbCo_2$; MER coordination	Only DC measurements; The magnetic coupling interactions between d-and f-metal ions in the series of [Fe–L1–Ln], [Co–L1–Ln] and [CoII–L2–Ln] coordination polymers were explicitly characterized.	45
25	ILUKAC	Heteropentametallic polimer – Yb_2Fe_3;	---	
26	JEVTUZ	Monometallic; MER coordination	---	87
27	JIWMUY	Heterohexametallic Yb_4Pt_2; MER coordination	---	88
28	KOLGIB	Monometallic – FAC coordination	---	89
29	KUNTIX	Monometallic – MER coordination; one bidentate axial nitrate, one axial and one equatorial water molecule, one equatorial and one axial DMF molecules	---	50
30	LAMFUA	Heterohexametalic polymeric material – Yb_4Ag_2; FAC coordination	---	90
31	MALLUG	Monometallic – MER coordination; two bidentate axial nitrates, one equatorial bidentate nitrate	---	91
32	METRUY	Monometallic – MER coordination; one bidentate axial nitrates, two equatorial H_2O molecules, two axial H_2O molecules	---	92
33	METSAF	Monometallic – MER coordination; two bidentate axial nitrates, monodentate equatorial nitrate, equatorial H_2O;	---	
34	NEYFED	Monometallic – MER coordination; two bidentate axial nitrates, one equatorial bidentate nitrate	---	93
35	NPYCYB	Monometallic – MER coordination;	---	94
36	PIRZUM	Monometallic – MER coordination; two bidentate axial nitrates, two equatorial water molecules	---	95
37	POVTIE	Heterotrimetallic: Yb_2Pt – MER coordination; three acetylacetonates (2 ax. 1 eq.)	---	96
38	PYCYBN	Monometallic – MER coordination;	---	97
39	QAKGIV	Monometallic; ion pair with POM; MER coordination	---	98
40	QAMBUE	Heterooctametallic; Yb_4Rb_4 – MER coordination	---	99
41	QAMCAL	Heterotrimetallic; Yb_2Rb – MER coordination	---	
42	QAMMEZ	Heterooctametallic coordination polymer; YbRb – MER coordination	---	
43	QEKXEK	Monometallic – MER coordination; two bidentate axial nitrates, one	---	100

		equatorial bidentate nitrate		
44	SAMFOD	Homobimetallic – MER coordination; three acetylacetonates (2 ax. 1 eq.)	---	101
45	SAMGAQ	Homobimetallic – MER coordination; three acetylacetonates (2 ax. 1 eq.)	---	
46	SPYCYB	Monometallic – MER coordination;	---	94
47	TOZLIF	Monometallic – MER coordination;	---	102
48	TUGYAW	Heterotrimetallic; Yb_2Rb – MER coordination;	---	59
49	UGUGUZ	Homotetrametallic polymeric assembly – MER coordination	---	61
50	VAJNEB	Heterooctametallic coordination polymers: Yb_2Cu_6 –MER coordination	---	64
51	XIDTEK	Monometallic – MER coordination	---	69
52	XITYOQ	Monometallic – MER coordination; ; two bidentate axial carboxylates, one equatorial monodentate carboxylate, one equatorial water molecule	---	70
53	YUMHAP	Monometallic (Cr-Yb ionic salt) – FAC coordination	---	72
54	ZIXHUE	Monometallic – MER coordination	Field-induced SIM; U_{eff} = 15.6 K; τ_0=2.73 10^{-6} s)	103

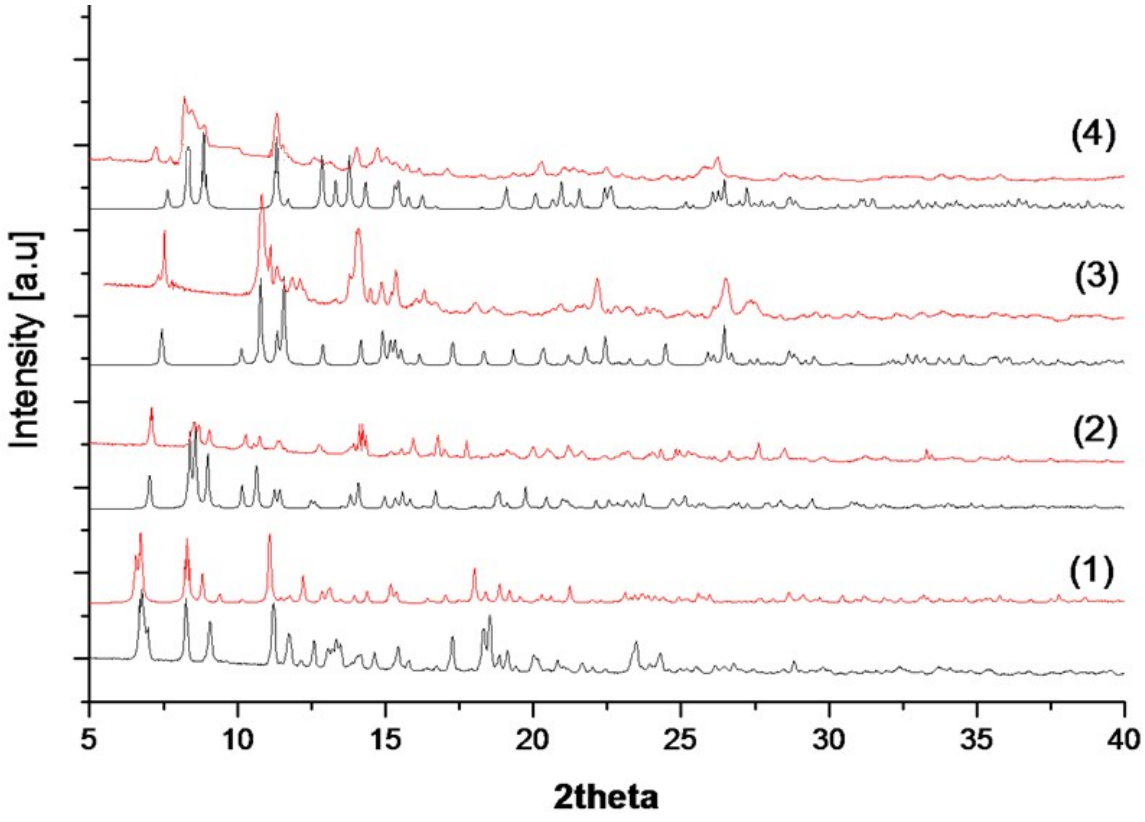

Fig. S1. Theoretical and experimental powder X-ray diffractograms obtained for compounds **1-4**.

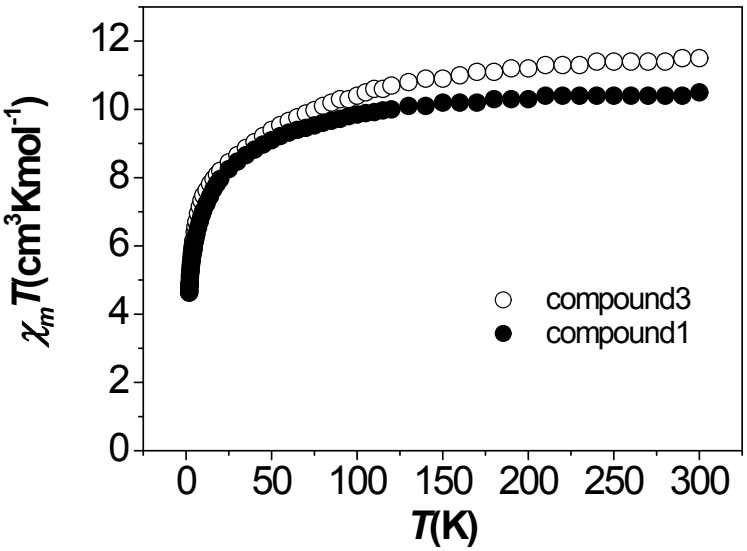

Fig. S2. Temperature dependence of the $\chi_m T$ product for compounds **1** and **3**.

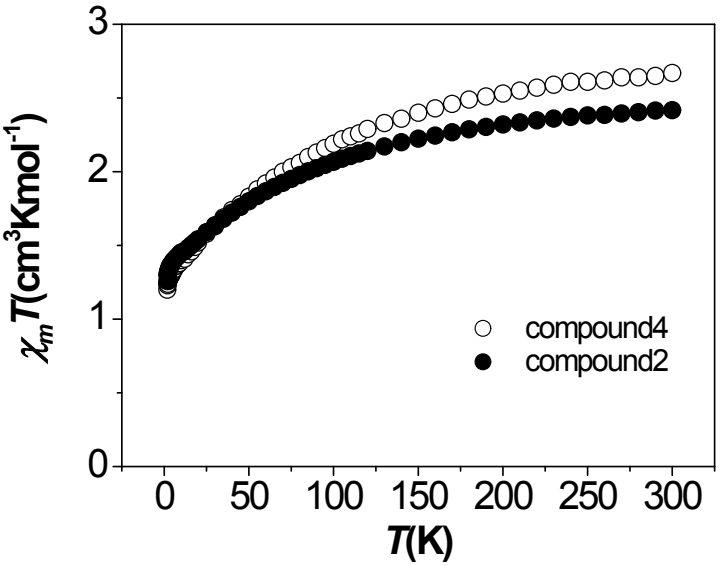

Fig. S3. Temperature dependence of the $\chi_m T$ product for compounds **2** and **4**.

Table S10. Comparison of DC magnetic data for **1 - 4** with the literature examples.

Compound, ion	Ground state of Ln(III), g-factor	Theoretical $\chi_m T$ [cm^3Kmol^{-1}][a]	Theoretical M_{sat} value [B.M.][b]	Experimental $\chi_m T_{(300K)}$/ $\chi_m T_{(1.8K)}$ [cm^3Kmol^{-1}]	Experimental M_{sat} value [B.M.]	Ref.
1, Er(III)	$^4I_{15/2}$, g=6/5	11.48	9	10.5/4.63	4.90	This work
3, Er(III)				11.5/4.64	5.17	
ITODOM Er(III)				10.38/7.34	5.35	6
ITOCUR Er(III)				13.04/5.7	4.23	
ITODIG Er(III)				11.29/5.39	5.29	
REJGUL Er(III)				11.3/6.0(4.5K)	4.28	104
2, Yb(III)	$^2F_{7/2}$, g_J=8/7	2.57	4	2.42/1.26	1.75	This work
4, Yb(III)				2.67/1.20	1.82	
ITODEC Yb(III)				2.21/1.99	1.94	6
ITODAY Yb(III)				2.24/1.44	1.74	
ITODUS Yb(III)				2.25/1.48	1.83	
REJHEW Yb(III)				2.31/1.26(4.5K)	1.72	104
MUFLOQ Yb(III)				2.32/1.13	1.85	105
MUFLUW Yb(III)				2.35/1.07	1.74	

[a] $\chi_m T=N\beta^2/3k\{g_J^2J(J+1)\}$, [b] $M=MJ\mu_B$; $J=L+S$; $g_J=3/2+S_T(S_T+1)-L(L+1)/2J(J+1)$

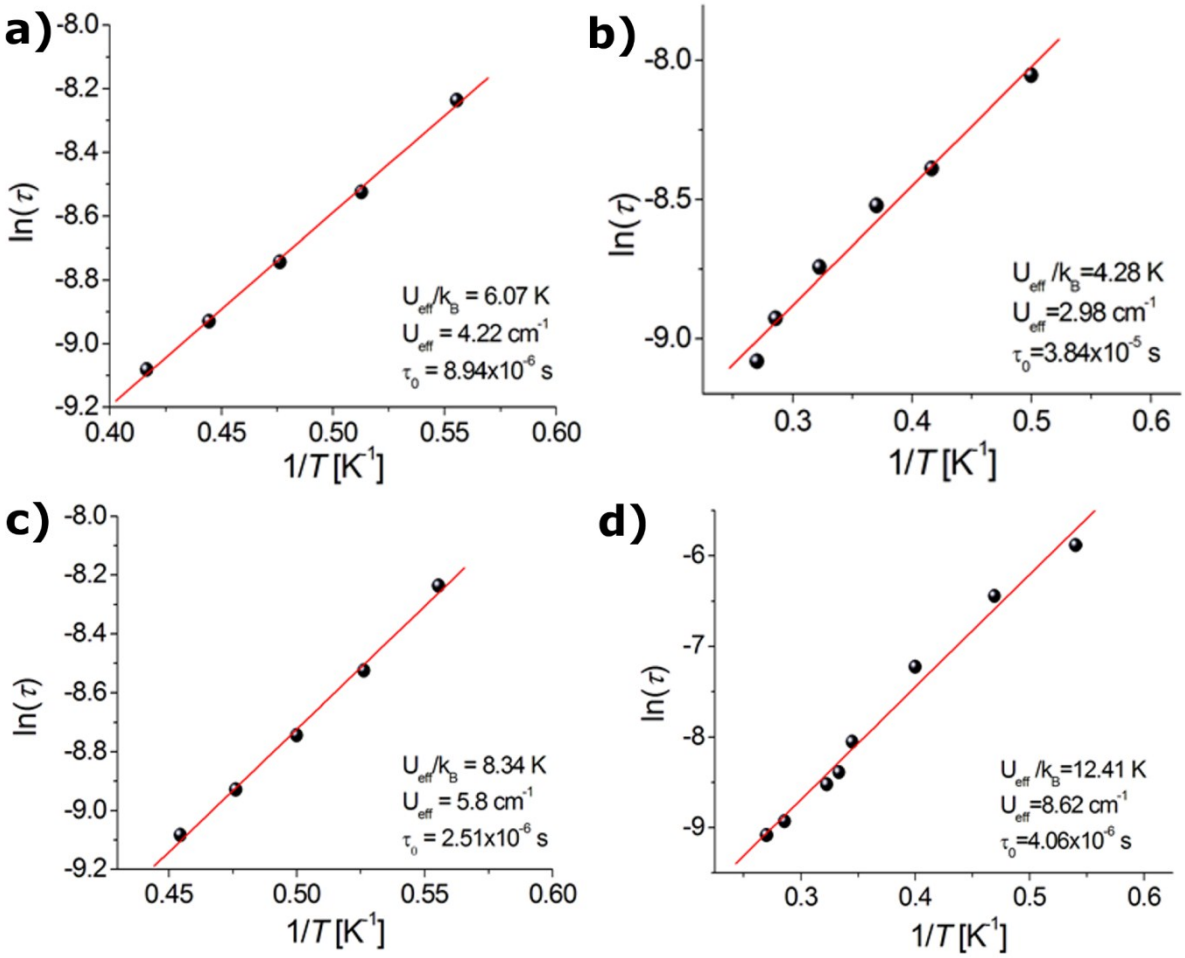

Fig. S4 Temperature dependence of the relaxation time for complexes **1** (a). **2** (b). **3** (c) and **4** (d). The solid line represents the Arrhenius law fit.

Table S11. Values of τ, α, χ_T and χ_s for complex **1** under a 0.1 T applied field and varying temperatures.

T **[K]**	**τ**	**α**	χ_T	χ_s	R^2
1.8	0.00025	0.1285	12.4453	0.7461	0.9887
2.0	0.00021	0.1286	11.9408	0.7647	0.9832
2.1	0.00016	0.1338	11.3518	0.6272	0.9799
2.2	0.00013	0.1427	10.8768	0.3428	0.9938
2.4	0.00010	0.1430	10.5285	0.2973	0.9805

Table. S12. Values of τ, α, χT and χs for complex **2** under a 0.1 T applied field and varying temperatures.

T **[K]**	**τ**	**α**	χ_T	χ_s	$\mathbf{R^2}$
2	0.00046	0.2574	1.8338	0.3583	0.9987
2.1	0.00043	0.2733	1.7609	0.3352	0.9780
2.3	0.00035	0.2740	1.6314	0.2949	0.9771
2.5	0.00030	0.2403	1.4943	0.3060	0.9789
2.7	0.00027	0.1982	1.3842	0.3283	0.9932
2.9	0.00023	0.1648	1.2838	0.3326	0.9899
3.1	0.00019	0.1332	1.2000	0.3354	0.9912
3.3	0.00017	0.1099	1.1306	0.3403	0.9931
3.5	0.00014	0.0820	1.0660	0.3444	0.9898
3.7	0.00011	0.0966	1.0105	0.3058	0.9763

Table. S13. Values of τ, α, χT and χs for complex **3** under a 0.1 T applied field and varying temperatures.

T **[K]**	**τ**	**α**	χ_T	χ_s	$\mathbf{R^2}$
1.8	0.00020	0.3406	16.8607	1.9725	0.9863
1.9	0.00018	0.3189	15.7250	2.2824	0.9730
2	0.00016	0.3230	14.9621	2.0472	0.9909
2.1	0.00016	0.2893	14.2572	2.5589	0.9819
2.2	0.00014	0.2918	13.7426	2.3381	0.9844

Table. S14. Values of τ, α, χ_T and χ_s for complex **4** under a 0.1 T applied field and varying temperatures.

T **[K]**	**τ**	**α**	χ_T	χ_s	$\mathbf{R^2}$
1.8	0.00220	0.1596	1.9818	0.3267	0.9962
1.9	0.00191	0.1666	1.8834	0.3062	0.9836
2.0	0.00165	0.1693	1.7970	0.2898	0.9917
2.1	0.00141	0.1674	1.7131	0.2749	0.9887
2.3	0.00105	0.1597	1.5803	0.2531	0.9782
2.5	0.00074	0.1528	1.4573	0.2351	0.9964
2.7	0.00052	0.1406	1.3500	0.2196	0.9993
2.9	0.00036	0.1400	1.2609	0.2028	0.9883
3.1	0.00026	0.1336	1.1818	0.1963	0.9781
3.3	0.00019	0.1292	1.1114	0.1841	0.9933
3.5	0.00014	0.1277	1.0510	0.1753	0.9940
3.7	0.00010	0.1256	0.9971	0.1719	0.9852

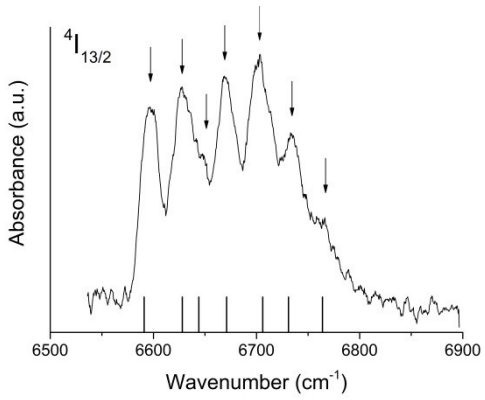
$^4I_{13/2}$
Absorbance (a.u.)
6500
6600
6700
6800
6900
Wavenumber (cm^{-1})

a)

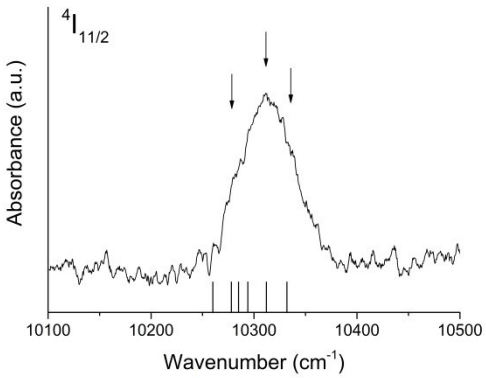
$^4I_{11/2}$
Absorbance (a.u.)
10100
10200
10300
10400
10500
Wavenumber (cm^{-1})

b)

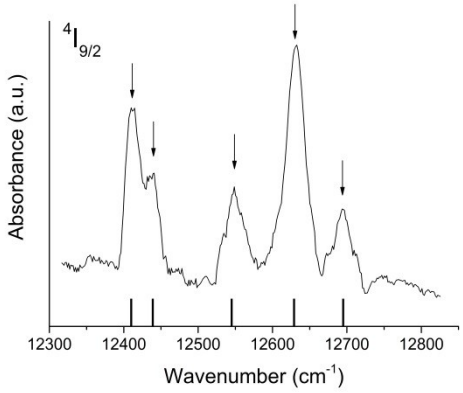
$^4I_{9/2}$
Absorbance (a.u.)
12300
12400
12500
12600
12700
12800
Wavenumber (cm^{-1})

c)

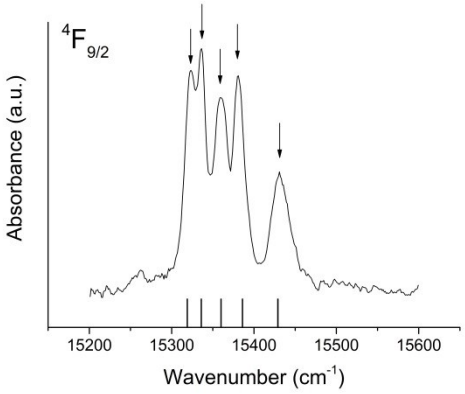
$^4F_{9/2}$
Absorbance (a.u.)
15200
15300
15400
15500
15600
Wavenumber (cm^{-1})

d)

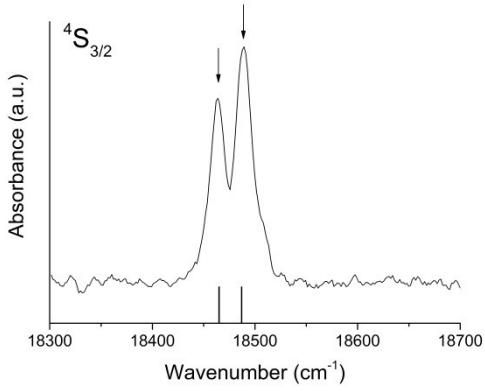
$^4S_{3/2}$
Absorbance (a.u.)
18300
18400
18500
18600
18700
Wavenumber (cm^{-1})

e)

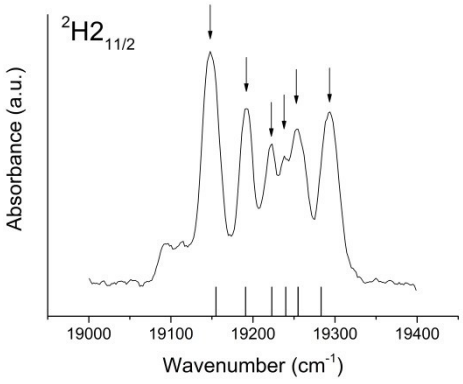
$^2H2_{11/2}$
Absorbance (a.u.)
19000
19100
19200
19300
19400
Wavenumber (cm^{-1})

f)

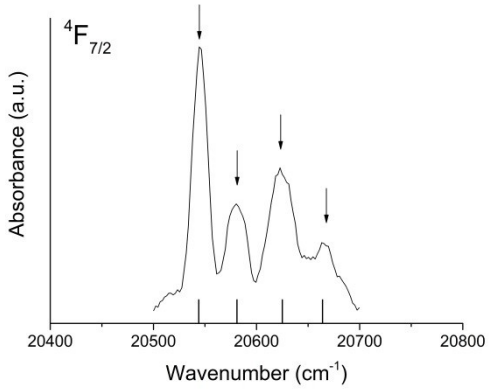

g)

Figure S5. Absorption spectra of Er(III) ion in compound **3** showing transitions from the ground multiplet $^4I_{15/2}$ to CF components of the excited multiplets: a) $^4I_{13/2}$, b) $^4I_{11/2}$, c) $^4I_{9/2}$, d) $^4F_{9/2}$, e) $^4S_{3/2}$, f) $^2H_{11/2}$, and g) $^4F_{7/2}$. Arrows and vertical bars indicate the experimental and calculated energy levels, respectively.

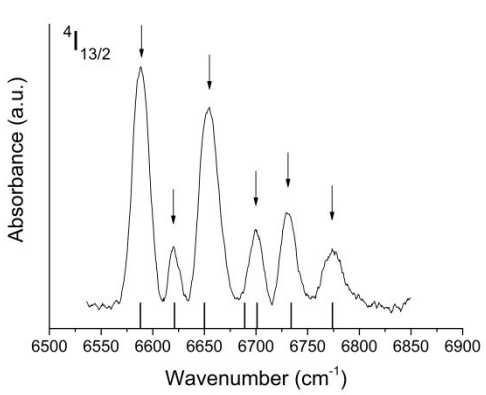

a)

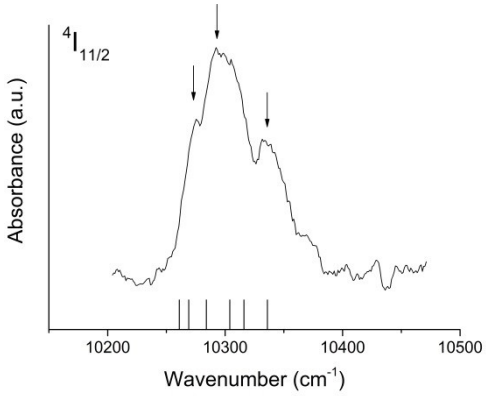

b)

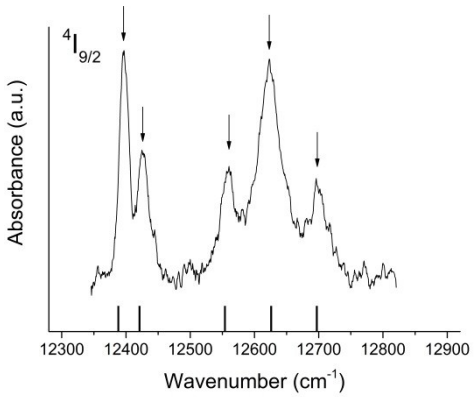

c)

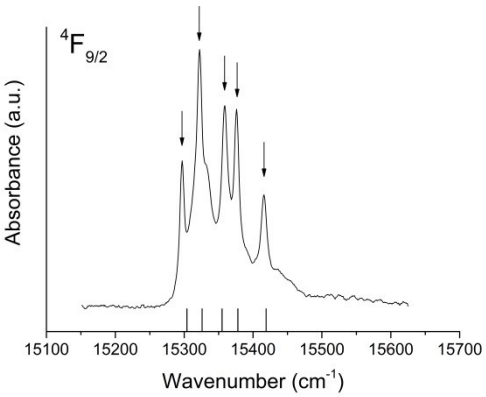

d)

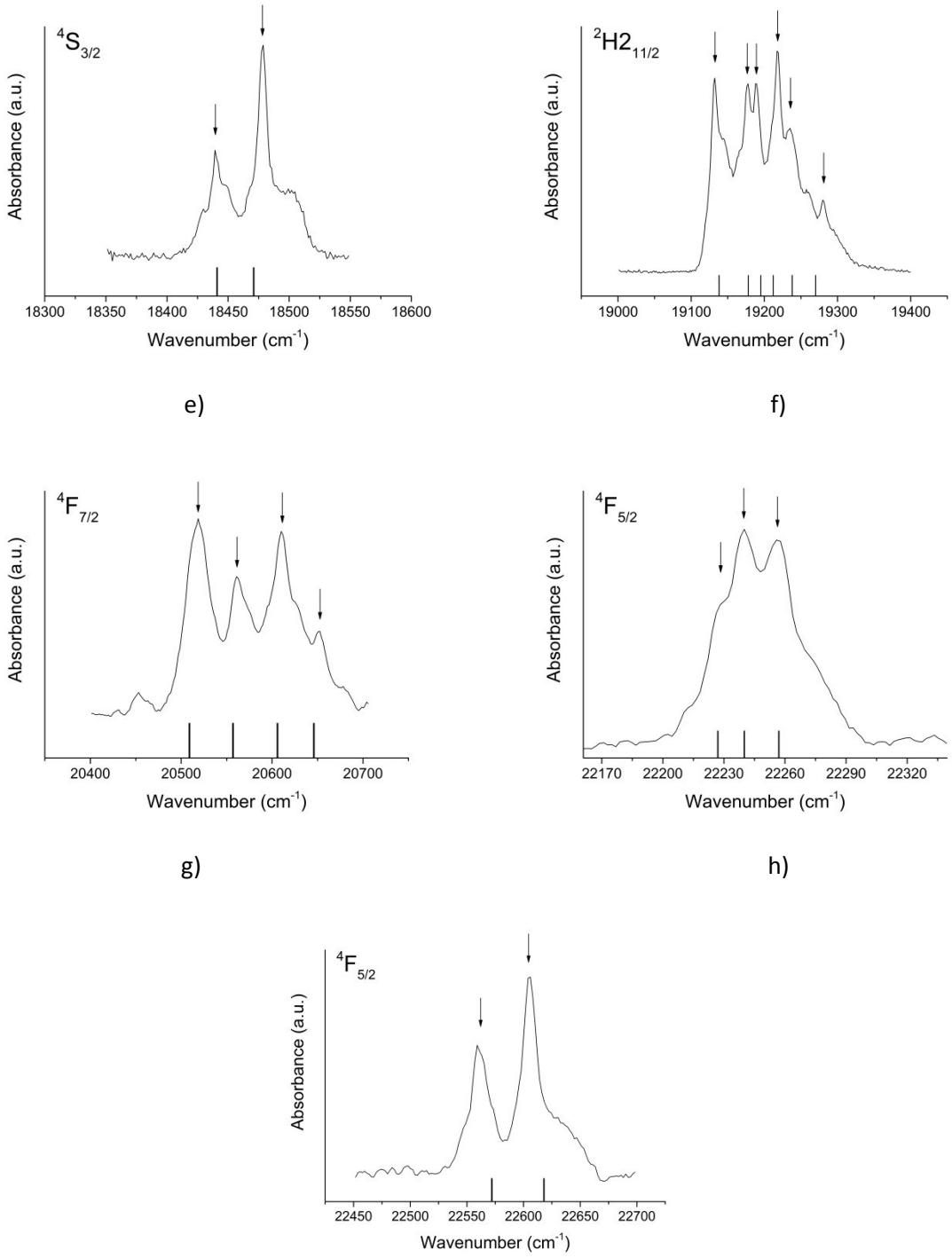

Figure S6. Absorption spectra of Er(III) ion in compound **3** showing transitions from the ground multiplet $^4I_{15/2}$ to CF components of the excited multiplets: a) $^4I_{13/2}$, b) $^4I_{11/2}$, c) $^4I_{9/2}$, d) $^4F_{9/2}$, e) $^4S_{3/2}$, f) $^2H_{11/2}$, g) $^4F_{7/2}$, h) $^4F_{5/2}$ and i) $^4F_{3/2}$. Arrows and vertical bars indicate the experimental and calculated energy levels, respectively.

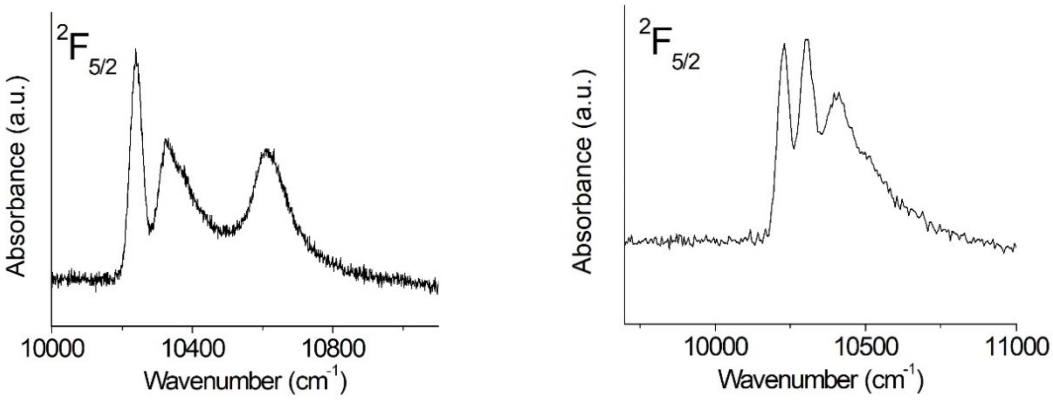

Fig. S7. Absorption spectra of Yb(III) ion in compound a) **2** and b) **4** showing transitions from the ground multiplet $^2F_{7/2}$ to CF components of the excited multiplet $^2F_{5/2}$.

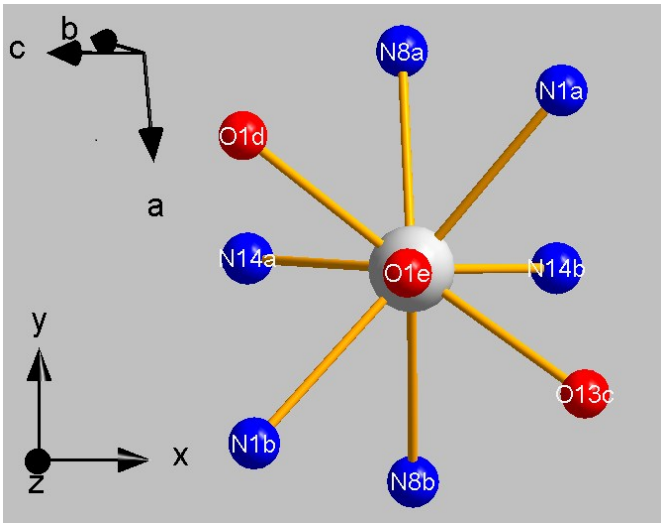

Fig. S8. Axis systems used for compound **1**: the original non-Cartesian crystallographic axis system (CAS) defined by the axes (*a*, *b*, *c*) and the modified Cartesian CAS (CAS*), i.e. the (*x*, *y*, *z*) coordinate system, selected so that the O1e atom is on the *z*-axis yielding the approximate C_2 axis and thus the approximated site symmetry C_2.

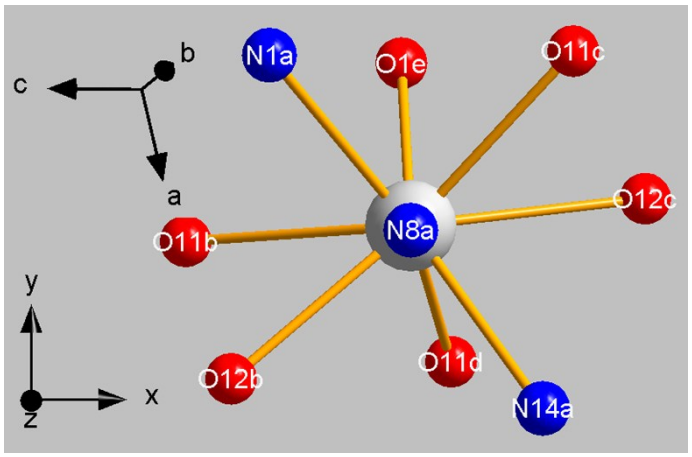

Fig. S9. Axis systems used for compound **3**: the original non-Cartesian crystallographic axis system (CAS) defined by the axes (*a*, *b*, *c*) and modified Cartesian CAS (CAS*), i.e. the (*x*, *y*, *z*) coordinate system, selected so that the N8A atom is on the *z*-axis yielding the approximate C_2 axis and thus the approximated site symmetry C_2.

Table S15. The calculated, approximated, and fitted CFPs for compound **1** and **3**; CFPs and *rms* values are in cm^{-1}. For explanations see main text.

CFPs	Compound **1**			Compound **3**		
Method	SPM-C_1	C_2 = rotation Oz/-32.3°	C_2 fit *rms* = 5.3	SPM-C_1	C_2 = rotation Oz/-20.42°	C_2 fit *rms* = 9.4
B_{20}	-35	-35	-14 ±62	-90	-90	58 ±68
ReB_{21}	73	0	0	-14	0	0
ImB_{21}	-32	0	0	156	0	0
ReB_{22}	44	103	126 ±31	-59	-78	-184 ±59
ImB_{22}	93	0	0	-51	0	0
B_{40}	98	98	-321 ±109	38	38	28 ±73
ReB_{41}	77	0	0	9	0	0
ImB_{41}	10	0	0	-26	0	0
ReB_{42}	165	-1	19 ±67	-244	-332	-6 ±75
ImB_{42}	-79	-183	-164 ±83	-226	-11	149 ±71
ReB_{43}	-40	0	0	-28	0	0
ImB_{43}	20	0	0	-28	0	0
ReB_{44}	-296	7	295 ±92	-147	166	321 ±33
ImB_{44}	-234	377	-246 ±87	189	173	33 ±65
B_{60}	338	338	301 ±78	488	488	477 ±113
ReB_{61}	75	0	0	80	0	0
ImB_{61}	-6	0	0	-35	0	0
ReB_{62}	413	199	-410 ±70	-370	-233	88 ±65
ImB_{62}	25	-363	-402 ±88	72	296	178 ±93
ReB_{63}	12	0	0	-257	0	0
ImB_{63}	-12	0	0	-130	0	0
ReB_{64}	532	-344	-397 ±62	307	318	338 ±112
ImB_{64}	-8	-406	89 ±68	277	-264	205 ±89
ReB_{65}	-107	0	0	-90	0	0
ImB_{65}	35	0	0	159	0	0
ReB_{66}	-90	142	-104 ±71	293	-236	301 ±61
ImB_{66}	-224	195	-141±81	-93	-197	-534 ±77

Table S16. Energy levels and components of the state vector for the ground multiplet $^4I_{15/2}$ of Er(III) in compound **1** obtained using the CFP set C_2-fit in Table S15.

Energy levels (in cm^{-1})	Composition of the wave functions (in %)							
	|±1/2>	|±3/2>	|±5/2>	|±7/2>	|±9/2>	|±11/2>	|±13/2>	|±15/2>
0	15	**24**	12	10	4	**21**	4	12
47	4	8	**24**	8	8	15	14	**18**
124	**44**	6	2	3	3	10	12	**20**
165	17	**17**	2	4	4	1	**56**	1
242	3	7	6	**25**	**39**	6	9	6
299	13	**25**	4	15	10	15	1	**16**
359	1	12	**45**	1	**29**	5	4	3
397	4	1	5	**35**	4	**27**		25

Table S17. Energy levels and components of the state vector for the ground multiplet $^4I_{15/2}$ of Er(III) in compound **3** obtained using the CFP set C_2-fit in Table S15.

Energy levels (in cm^{-1})	Composition of the wave functions (in %)							
	|±1/2>	|±3/2>	|±5/2>	|±7/2>	|±9/2>	|±11/2>	|±13/2>	|±15/2>
0	31	16	2	1	8	**23**	**18**	2
38	2	17	**30**	13	6	6	**27**	1
122	9	**15**	3	**15**	9	13	**25**	11
195	**24**	13	5	**14**	13	9	8	**14**
256	**25**	0	5	10	15	**26**	16	3
305	4	7	**22**	0	3	10	4	**50**
365	5	**30**	1	3	**42**	11	1	8
441	1	3	**32**	**44**	5	2	3	10

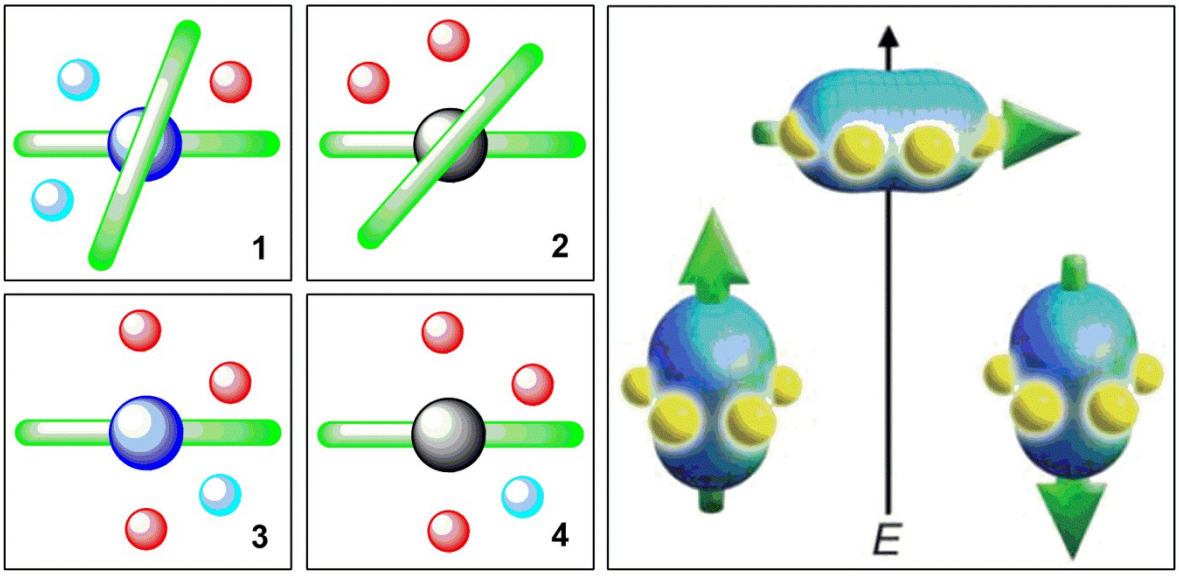

Fig. S10. Schematic representation of compounds **1-4** based on their single crystal X-ray measurements confronted with the model proposed by Long and co-workers. Adapted with permission from ref [1] Copyright 2011 Royal Society of Chemistry.

Comment 1: Additional comments on the computational procedure and the C_2 symmetry approximation.

An alternative procedure for reduction of the CFP sets corresponding to the actual C_1 (triclinic) symmetry to the CFP sets corresponding to the approximated C_2 (monoclinic) symmetry is based on the diagonalization of the second-rank crystal field terms for $3d^N$ and $4f^N$ ions at triclinic or monoclinic symmetry sites (the 3DD method).[106] Importantly, one rotation about the Oz axis cannot reduce all three non-orthorhombic CFPs: ReB_{21}, ImB_{21} and ImB_{22} to zero. This can be achieved only using the 3DD method, which handles two rotations that are needed in this case.

However, the procedure for the C_2 symmetry approximation used in the present calculations should be seen before any 3DD rotations. The approximate C_2 axis appears for such axis system orientation as shown in Fig. S8 and S9. After the 3DD rotations a completely different orientation of the axis system would be obtained. In other words, we do not implement the C_2 symmetry approximation by resetting the CFPs ReB_{21}, ImB_{21} and ImB_{22} to zero via the 3DD rotations but by neglecting those CFPs that should be zero for the C_2 symmetry. Thus, we neglect ReB_{21} and ImB_{21}, whereas only ImB_{22} is reset by appropriate rotation, which that does not change the orientation of the *z*-axis. Hence in this case the approximate C_2 axis is preserved. This procedure is analogous to SPM calculations of the geometric coefficients g_{kq} for C_1 symmetry, which would yield the triclinic ones being small, thus justifying their neglect. Here we just went one step further. First, we have fitted the SPM intrinsic parameters and then taken for further calculations only the so-obtained non-triclinic CFPs. Therefore, the triclinic CFPs are not listed in Table S15 since for the C_2 symmetry they do not appear.

Comment 2: Additional comments on the results for compound 2 and 4.

For Yb compounds **2** and **4** the absorption spectra do not provide sufficient data to perform full scale CF calculations. Hence we have performed only suitable simulations and calculated the expected splitting of the ground multiplet $^2F_{7/2}$ of Yb(III) ion for compound **2** and **4** taking directly the CFPs obtained for erbium compounds **1** and **3**, respectively. Note that since no suitable rescaling relationships[107] exist we cannot consider rescaling of Er-CFPs to obtain more reliable CFPs for Yb. So-obtained calculated splitting of the ground multiplet $^2F_{7/2}$ of Yb(III) ion is 0, 128, 198 and 307 for compound **2**, whereas 0, 120, 237 and 295 for compound **4**. For compound **2** the composition of the state vector for the ground and first excited level is {52% |5/2> + 31% |1/2> + 11% |-3/2>+ 6% |-7/2>} and {28% |5/2> + 15% |1/2> + 1% |-3/2>+ 56% |-7/2>}, respectively. Correspondingly, for compound **4** we obtain {44% |5/2> + 27% |1/2> + 21% |-3/2>+ 8% |-7/2>} and {11% |5/2> + 46% |1/2> + 2% |-3/2>+41% |-7/2>}. These tentative results serve only for illustration of potential effectiveness of the methods employed. However, since their reliability may be doubtful they do not allow for meaningful correlation of the spectroscopic data and magnetic susceptibility measurements.

Comment 3: Theoretical background.

For the energy level calculations we apply the effective operator model suitable for $4f^N$ ions in crystal.[108-112] The observed energy levels are fitted to the phenomenological Hamiltonian, $\hat{H} = \hat{H}_{FI} + \hat{H}_{CF}$, by simultaneous diagonalization of the two parts - the free-ion ($\hat{H}_{FI}$) Hamiltonian:

$$\hat{H}_{FI} = E_{ave} + \sum_{k=2,4,6} F^k(nf,nf)\hat{f}_k + \zeta_{4f}\hat{A}_{SO} + \alpha\hat{L}(\hat{L}+1) + \beta\hat{G}(G_2) + \gamma\hat{G}(R_7) + \sum_{i=2,3,4,6,7,8} T^i\hat{t}_i + \sum_{j=0,2,4} M^j\hat{m}_j + \sum_{k=2,4,6} P^k\hat{p}_k \quad , \qquad (1)$$

and the crystal-field Hamiltonian ($\hat{H}_{CF}$) expressed in the compact form[113-115] in the Wybourne notation[108]:

$$\hat{H}_{CF} = \sum_{k,q} B_{kq}\hat{C}_q^{(k)}(x,y,z) . \qquad (2)$$

The operators and interaction parameters in Eq. (1) as well as the intra-configurational spherical-tensor operators $\hat{C}_q^{(k)}$, expressed in a given axis system (*x*, *y*, *z*), and the *symbolic* CFPs[116, 117] B_{kq}, of rank *k* and component *q*, in Eq. (2) are defined according to the prevailing conventions. [108-111] In low symmetry CFP studies, the expanded form of $\hat{H}_{CF}$ is most often used, in which the *Re* and *Im* parts of the complex CFPs in Eq. (2) are explicitly indicated: $B_{kq} = \mathrm{Re}\,B_{kq} + i\,\mathrm{Im}\,B_{kq}$. Due to properties of the Wybourne operators[108]: $B_{k-q} = (-1)^q B_{kq}^*$ (see, e.g. [111, 118]) the relations hold: $Re\,B_{k-q} = (-1)^q Re\,B_{kq}$, $Im\,B_{k-q} = (-1)^{q+1} Im\,B_{kq}$.

If the central ion site has no symmetry elements, i.e. for triclinic symmetry, according to group theory all 27 CFPs B_{kq} in Eq. (2) are non-zero, including 3 real B_{k0} (k = 2, 4, 6) and 24 complex CFPs, which are interdependent 'in-pairs' with (+q, -q). In general, for monoclinic (C_2, C_s, or C_{2h}) site symmetry three possible forms of $\hat{H}_{CF}$ exist[119], each corresponding to a specific choice of the monoclinic axis (or direction) as the *z*-, *y*-, or *x*-axis.[116, 118] The axis system adopted here corresponds to the case most often used in literature, i.e. $C_2||z$. It yields the non-zero CFPs ReB_{kq} and $Im\ B_{kq}$ with q even only, whereas the number of CFPs is reduced from 27 to 15; the explicit $\hat{H}_{CF}$ forms may be found, in e.g.[120, 121]. In addition, parameter ImB_{22} can be put to zero by appropriate rotation of axis system which leaves 14 independent CFPs.

To reduce the number of parameters at initial stages of fittings the superposition model (SPM) was employed, which is based on the main assumption that the CFPs for a central metal ion may be expressed as a sum of cylindrically symmetric single-ligand (L) contributions.[122-124] The SPM expressions expressed consistently in the Wybourne notation[108] are:

$$Re\,B_{kq} = \sum_L \overline{B}_k(R_L) g_{k,q}(\theta_L,\varphi_L) ,$$

$$Im\,B_{kq} = \sum_L \overline{B}_k(R_L) g_{k,-q}(\theta_L, \varphi_L)\,, \tag{4}$$

where $\overline{B}_k$ are the intrinsic parameters and $g_{k,q}$ are the coordination factors.

In the SPM model the distance dependence is assumed in the form of a power law with the coefficients t_k [121-123]:

$$\overline{B}_k(R\ ) = \overline{B}_k(R_0)(R_0/R)^{t_k}\,, \tag{5}$$

where R_0 is usually assumed to be the average metal-ligand distance. Eq. (4) may be than rewritten as:

$$Re\,B_{kq} = \sum_L \overline{B}_k(R_0)\left(R_0/R_L\right)^{t_k} g_{k,q}(\theta_L, \varphi_L) \tag{6}$$

$$Im\,B_{kq} = \sum_L \overline{B}_k(R_0)\left(R_0/R_L\right)^{t_k} g_{k,-q}(\theta_L, \varphi_L)\,.$$

References:

1. J. D. Rinehart and J. R. Long, *Chem. Sci.*, 2011, **2**, 2078-2085.
2. N. André, T. B. Jensen, R. Scopelliti, D. Imbert, M. Elhabiri, G. Hopfgartner, C. Piguet and J.-C. G. Bünzli, *Inorg. Chem.*, 2004, **43**, 515-529.
3. A. Gorczynski, M. Kubicki, D. Pinkowicz, R. Pelka, V. Patroniak and R. Podgajny, *Dalton Trans.*, 2015, **44**, 16833-16839.
4. L. Valencia, J. Martinez, A. Macías, R. Bastida, R. A. Carvalho and C. F. G. C. Geraldes, *Inorg. Chem.*, 2002, **41**, 5300-5312.
5. S. Quici, G. Marzanni, A. Forni, G. Accorsi and F. Barigelletti, *Inorg. Chem.*, 2004, **43**, 1294-1301.
6. J.-R. Jiménez, I. F. Díaz-Ortega, E. Ruiz, D. Aravena, S. J. A. Pope, E. Colacio and J. M. Herrera, *Chem. Eur. J.*, 2016, **22**, 14548-14559.
7. K. A. Thiakou, V. Nastopoulos, A. Terzis, C. P. Raptopoulou and S. P. Perlepes, *Polyhedron*, 2006, **25**, 539-549.
8. A. Gerus, K. Ślepokura and J. Lisowski, *Inorg. Chem.*, 2013, **52**, 12450-12460.
9. J. E. Cosgriff, G. B. Deacon, G. D. Fallon, B. M. Gatehouse, H. Schumann and R. Weimann, *Chem. Ber.*, 1996, **129**, 953-958.
10. G. L. Guillet, I. F. D. Hyatt, P. C. Hillesheim, K. A. Abboud and M. J. Scott, *New J. Chem.*, 2013, **37**, 119-131.
11. A. Rodríguez-Rodríguez, D. Esteban-Gómez, A. de Blas, T. Rodríguez-Blas, M. Fekete, M. Botta, R. Tripier and C. Platas-Iglesias, *Inorg. Chem.*, 2012, **51**, 2509-2521.
12. C. Tang, F. Wang, R. Chen, W. Jiang, Y. Zhang and D. Jia, *J. Solid State Chem.*, 2013, **204**, 70-77.
13. M. A. J. Moss, C. J. Jones and A. J. Edwards, *Polyhedron*, 1988, **7**, 79-81.
14. M. A. J. Moss, C. J. Jones and A. J. Edwards, *J. Chem. Soc. Dalton Trans.*, 1989, DOI: 10.1039/DT9890001393, 1393-1400.
15. T. Sanada, T. Suzuki, T. Yoshida and S. Kaizaki, *Inorg. Chem.*, 1998, **37**, 4712-4717.
16. J. Wang, H. Li, P. Chen, M. Zhang, W. Sun and P. Yan, *Z. Anorg. Allg. Chem.*, 2016, **642**, 368-371.
17. M. A. J. Moss and C. J. Jones, *Polyhedron*, 1989, **8**, 117-119.

18. M. A. J. Moss and C. J. Jones, *J. Chem. Soc. Dalton Trans.*, 1990, 581-591.
19. S. Beaini, G. B. Deacon, E. E. Delbridge, P. C. Junk, B. W. Skelton and A. H. White, *Eur. J. Inorg. Chem.*, 2008, **2008**, 4586-4596.
20. G. B. Deacon, P. C. Junk and D. Werner, *Polyhedron*, 2016, **103, Part A**, 178-186.
21. S. Beaini, G. B. Deacon, C. M. Forsyth and P. C. Junk, *Z. Anorg. Allg. Chem.*, 2008, **634**, 2903-2906.
22. S. Petoud, J.-C. G. Bünzli, F. Renaud, C. Piguet, K. J. Schenk and G. Hopfgartner, *Inorg. Chem.*, 1997, **36**, 5750-5760.
23. M. Abdus Subhan, R. Kawahata, H. Nakata, A. Fuyuhiro, T. Tsukuda and S. Kaizaki, *Inorganica Chim. Acta*, 2004, **357**, 3139-3146.
24. N. Yuushou, N. Akira and M. Kazushi, *Chem. Lett.*, 1997, **26**, 803-804.
25. H. He and A. G. Sykes, *Inorg. Chem. Commun.*, 2008, **11**, 1304-1307.
26. T. Sanada, T. Suzuki and S. Kaizaki, *J. Chem. Soc. Dalton Trans.*, 1998, DOI: 10.1039/A706834D, 959-966.
27. H. C. Aspinall, J. F. Bickley, N. Greeves, R. V. Kelly and P. M. Smith, *Organometallics*, 2005, **24**, 3458-3467.
28. M. A. Subhan, T. Suzuki and S. Kaizaki, *J. Chem. Soc. Dalton Trans.*, 2001, DOI: 10.1039/B007369P, 492-497.
29. H. He, M. Dubey, A. G. Sykes and P. S. May, *Dalton Trans.*, 2010, **39**, 6466-6474.
30. H. He, A. G. Sykes, P. S. May and G. He, *Dalton Trans.*, 2009 , 7454-7461.
31. H. Zhou, Q. Chen, H.-B. Zhou, X.-Z. Yang, Y. Song and A.-H. Yuan, *Cryst. Growth Des.*, 2016, **16**, 1708-1716.
32. J. Gregoliński, K. Ślepokura and J. Lisowski, *Inorg. Chem.*, 2007, **46**, 7923-7934.
33. Y. Inomata, T. Sunakawa and F. S. Howell, *J. Mol. Struct.*, 2003, **648**, 81-88.
34. Y. Fukuda, A. Nakao and K. Hayashi, *J. Chem. Soc. Dalton Trans.*, 2002, 527-533.
35. F. Wang, Y. Sun, Y. Zhao and S. Wu, *Synth. React. Inorg. M.*, 2009, **39**, 225-229.
36. M. G. B. Drew, M. J. Hudson, P. B. Iveson, C. Madic and M. L. Russell, *J. Chem. Soc. Dalton Trans.*, 1999, 2433-2440.
37. M. Kozłowski, R. Kierzek, M. Kubicki and W. Radecka-Paryzek, *J. Inorg. Biochem.*, 2013, **126**, 38-45.
38. B. Zhao, X. Q. Zhao, Z. Chen, W. Shi, P. Cheng, S. P. Yan and D. Z. Liao, *CrystEngComm*, 2008, **10**, 1144-1146.
39. M. G. B. Drew, M. J. Hudson, P. B. Iveson, C. Madic and M. L. Russell, *J. Chem. Soc. Dalton Trans.*, 2000, 2711-2720.
40. Q. Mei and B. Tong, *Acta Crystallogr., Sect. E: Struct. Rep. Online*, 2010, **66**, m106-m106.
41. J. Fan, Z.-H. Wang, Z.-F. Huang, X. Yin and W.-G. Zhang, *Inorg. Chem. Commun.*, 2010, **13**, 659-662.
42. S. A. Cotton and P. R. Raithby, *Inorg. Chem. Commun.*, 1999, **2**, 86-88.
43. B.-L. An, J. Song, K.-W. Cheah, Y.-Y. Ren and Z.-X. Cheng, *Inorganica Chim. Acta*, 2009, **362**, 3196-3200.
44. B. E. Aroussi, S. Zebret, C. Besnard, P. Perrottet and J. Hamacek, *J. Am. Chem. Soc.*, 2011, **133**, 10764-10767.
45. X.-Q. Zhao, P. Cui, B. Zhao, W. Shi and P. Cheng, *Dalton Trans.*, 2011, **40**, 805-819.
46. M. J. Hudson, M. G. B. Drew, M. R. S. Foreman, C. Hill, N. Huet, C. Madic and T. G. A. Youngs, *Dalton Trans.*, 2003, 1675-1685.
47. P. Comba, M. Großhauser, R. Klingeler, C. Koo, Y. Lan, D. Müller, J. Park, A. Powell, M. J. Riley and H. Wadepohl, *Inorg. Chem.*, 2015, **54**, 11247-11258.
48. R. C. Palenik, K. A. Abboud, S. P. Summers, L. L. Reitfort and G. J. Palenik, *Inorganica Chim. Acta*, 2006, **359**, 4645-4650.
49. C. R. De Silva, J. R. Maeyer, A. Dawson and Z. Zheng, *Polyhedron*, 2007, **26**, 1229-1238.
50. M. Stojanovic, N. J. Robinson, X. Chen, P. A. Smith and R. E. Sykora, *J. Solid State Chem.*, 2010, **183**, 933-939.

51. C. Cheng, H.-L. Gao and P. Cheng, *Chin. J. Inorg. Chem.*, 2004, **20**, 1237-1240.
52. V. N. Serezhkin, A. V. Vologzhanina, L. B. Serezhkina, E. S. Smirnova, E. V. Grachova, P. V. Ostrova and M. Y. Antipin, *Acta Crystallogr.,Sect.B:Struct.Sci.*, 2009, **65**, 45-53.
53. Jack M. Harrowfield, George A. Koutsantonis, Brian W. Skelton, Adam J. Strong and Allan H. White, *Z. Anorg. Allg. Chem.*, 2010, **636**, 808-817.
54. P. A. Brayshaw, A. K. Hall, W. T. A. Harrison, J. M. Harrowfield, D. Pearce, T. M. Shand, B. W. Skelton, C. R. Whitaker and A. H. White, *Eur. J. Inorg. Chem.*, 2005, **2005**, 1127-1141.
55. Y. Chen, S. She, L. Zheng, B. Hu, W. Chen, B. Xu, Z. Chen, F. Zhou and Y. Li, *Polyhedron*, 2011, **30**, 3010-3016.
56. K. A. Thiakou, V. Bekiari, C. P. Raptopoulou, V. Psycharis, P. Lianos and S. P. Perlepes, *Polyhedron*, 2006, **25**, 2869-2879.
57. P. M. Haba, F. B. Tamboura, O. Diouf, M. Gaye, A. S. Sall, C. A. Balde and C. Slebodnick, *Bull.Chem.Soc.Ethiop.* , 2006, **20**, 45-54.
58. F. B. Tamboura, O. Diouf, A. H. Barry, M. Gaye and A. S. Sall, *Polyhedron*, 2012, **43**, 97-103.
59. M. Albrecht, O. Osetska, J.-C. G. Bünzli, F. Gumy and R. Fröhlich, *Chemistry – A European Journal*, 2009, **15**, 8791-8799.
60. B. Zhao, P. Cheng, Y. Dai, C. Cheng, D.-Z. Liao, S.-P. Yan, Z.-H. Jiang and G.-L. Wang, *Angew. Chem. Int. Ed.*, 2003, **42**, 934-936.
61. Y.-P. Quan, L.-H. Zhao, A.-H. Yang, J.-Z. Cui, H.-L. Gao, F.-L. Lu, W. Shi and P. Cheng, *CrystEngComm*, 2009, **11**, 1679-1685.
62. L. Babel, T. N. Y. Hoang, L. Guénée, C. Besnard, T. A. Wesolowski, M. Humbert-Droz and C. Piguet, *Chem. Eur. J.*, 2016, **22**, 8113-8123.
63. G. M. de Oliveira, A. Machado, G. W. Gomes, J. H. S. K. Monteiro, M. R. Davolos, U. Abram and A. Jagst, *Polyhedron*, 2011, **30**, 851-859.
64. Q.-B. Bo, G.-X. Sun and D.-L. Geng, *Inorg. Chem.*, 2010, **49**, 561-571.
65. P. Chen, M. Zhang, W. Sun, H. Li, L. Zhao and P. Yan, *CrystEngComm*, 2015, **17**, 5066-5073.
66. H.-L. Gao, B. Zhao, X.-Q. Zhao, Y. Song, P. Cheng, D.-Z. Liao and S.-P. Yan, *Inorg. Chem.*, 2008, **47**, 11057-11061.
67. L. I. Semenova and A. H. White, *Aust. J. Chem.*, 1999, **52**, 539-550.
68. G. Bozoklu, C. Marchal, J. Pecaut, D. Imbert and M. Mazzanti, *Dalton Trans.*, 2010, **39**, 9112-9122.
69. M. Albrecht, O. Osetska, J. Klankermayer, R. Frohlich, F. Gumy and J.-C. G. Bunzli, *Chem. Commun.*, 2007, 1834-1836.
70. K. P. Carter, S. J. A. Pope and C. L. Cahill, *CrystEngComm*, 2014, **16**, 1873-1884.
71. A. S. R. Chesman, D. R. Turner, K. J. Berry, N. F. Chilton, B. Moubaraki, K. S. Murray, G. B. Deacon and S. R. Batten, *Dalton Trans.*, 2012, **41**, 11402-11412.
72. J. Harrowfield, Y. Kim, B. Skelton and A. White, *Aust. J. Chem.*, 1995, **48**, 807-823.
73. Y. Chen, Y. Cao, Y. Li and W. Liu, *Chin. J. Struct. Chem.*, 2013, **32**, 1859-1867.
74. M. G. B. Drew, C. Hill, M. J. Hudson, P. B. Iveson, C. Madic and T. G. A. Youngs, *Dalton Trans.*, 2004, 244-251.
75. M. Rafizadeh, M. Ranjbar and V. Amani, *Acta Crystallogr., Sect. E: Struct. Rep. Online*, 2004, **60**, m479-m481.
76. S. Zebret, C. Besnard, G. Bernardinelli and J. Hamacek, *Eur. J. Inorg. Chem.*, 2012, **2012**, 2409-2417.
77. M. Albrecht, O. Osetska, R. Fröhlich, J.-C. G. Bünzli, A. Aebischer, F. Gumy and J. Hamacek, *J. Am. Chem. Soc.*, 2007, **129**, 14178-14179.
78. M. Feng, S. Speed, F. Pointillart, B. Lefeuvre, B. Le Guennic, S. Golhen, O. Cador and L. Ouahab, *Eur. J. Inorg. Chem.*, 2016, **2016**, 2039-2050.
79. B. Ahrens, S. A. Cotton, N. Feeder, O. E. Noy, P. R. Raithby and S. J. Teat, *J. Chem. Soc. Dalton Trans.*, 2002, 2027-2030.
80. B. Zhao, P. Cheng, X. Chen, C. Cheng, W. Shi, D. Liao, S. Yan and Z. Jiang, *J. Am. Chem. Soc.*, 2004, **126**, 3012-3013.

81. E. Terazzi, S. Torelli, G. Bernardinelli, J.-P. Rivera, J.-M. Bénech, C. Bourgogne, B. Donnio, D. Guillon, D. Imbert, J.-C. G. Bünzli, A. Pinto, D. Jeannerat and C. Piguet, *J. Am. Chem. Soc.*, 2005, **127**, 888-903.
82. H. Katsura, N. Noriharu, H. Kazumasa, H. Masa-aki and F. Yutaka, *Chem. Lett.*, 1998, **27**, 1173-1174.
83. J. M. Bakker, G. B. Deacon and P. C. Junk, *Polyhedron*, 2013, **52**, 560-564.
84. J. Wang, X.-D. Zhang, Z.-R. Liu and W.-G. Jia, *J. Mol. Struct.*, 2002, **613**, 189-193.
85. K. T. Hua, J. Xu, E. E. Quiroz, S. Lopez, A. J. Ingram, V. A. Johnson, A. R. Tisch, A. de Bettencourt-Dias, D. A. Straus and G. Muller, *Inorg. Chem.*, 2012, **51**, 647-660.
86. G. Kervern, A. D'Aléo, L. Toupet, O. Maury, L. Emsley and G. Pintacuda, *Angew. Chem. Int. Ed.*, 2009, **48**, 3082-3086.
87. P. Xiangyang, Y. Shiping, W. Genglin, W. Honggen, W. Ruji and Y. Xinkan, *Acta Chimica Sinica*, 1989, **47**, 795-799.
88. X.-L. Li, L.-X. Shi, L.-Y. Zhang, H.-M. Wen and Z.-N. Chen, *Inorg. Chem.*, 2007, **46**, 10892-10900.
89. Kenneth I. Hardcastle, M. Botta, M. Fasano and G. Digilio, *Eur. J. Inorg. Chem.*, 2000, **2000**, 971-977.
90. C. Brouca-Cabarrecq, O. Fava and A. Mosset, *J. Chem. Cryst.*, 1999, **29**, 81-86.
91. M. G. B. Drew, P. B. Iveson, M. J. Hudson, J. O. Liljenzin, L. Spjuth, P.-Y. Cordier, A. Enarsson, C. Hill and C. Madic, *J. Chem. Soc. Dalton Trans.*, 2000, 821-830.
92. N. Boubals, M. G. B. Drew, C. Hill, M. J. Hudson, P. B. Iveson, C. Madic, M. L. Russell and T. G. A. Youngs, *J. Chem. Soc. Dalton Trans.*, 2002, 55-62.
93. E. Terazzi, L. Guénée, P.-Y. Morgantini, G. Bernardinelli, B. Donnio, D. Guillon and C. Piguet, *Chem. Eur. J.*, 2007, **13**, 1674-1691.
94. J. Albertsson, *Acta Chem.Scand.*, 1972, **26**, 1023-1044.
95. I. A. Charushnikova and C. den Over, *Cryst. Rep.*, 2006, **51**, 982-987.
96. H.-B. Xu, L.-Y. Zhang, X.-M. Chen, X.-L. Li and Z.-N. Chen, *Cryst. Growth Des.*, 2009, **9**, 569-576.
97. J. Albertsson, *Acta Chemica Scandinavica*, 1970, **24**, 1213-1229.
98. P. G. Reddy, N. Mamidi and C. P. Pradeep, *CrystEngComm*, 2016, **18**, 4272-4276.
99. W. Chen, X. Tang, W. Dou, Z. Ju, B. Xu, W. Xu and W. Liu, *Chem. Commun.*, 2016, **52**, 5124-5127.
100. R. F. Ziessel, G. Ulrich, L. Charbonnière, D. Imbert, R. Scopelliti and J.-C. G. Bünzli, *Chem. Eur. J.*, 2006, **12**, 5060-5067.
101. J.-F. Lemonnier, L. Guénée, C. Beuchat, T. A. Wesolowski, P. Mukherjee, D. H. Waldeck, K. A. Gogick, S. Petoud and C. Piguet, *J. Am. Chem. Soc.*, 2011, **133**, 16219-16234.
102. D. Kumar and A. Ramana, *CSD Communication*, 2014.
103. X. Yi, K. Bernot, V. Le Corre, G. Calvez, F. Pointillart, O. Cador, B. Le Guennic, J. Jung, O. Maury, V. Placide, Y. Guyot, T. Roisnel, C. Daiguebonne and O. Guillou, *Chem. Eur. J.*, 2014, **20**, 1569-1576.
104. I. Oyarzabal, B. Artetxe, A. Rodriguez-Dieguez, J. A. Garcia, J. M. Seco and E. Colacio, *Dalton Trans.*, 2016, **45**, 9712-9726.
105. Q.-W. Li, J.-L. Liu, J.-H. Jia, Y.-C. Chen, J. Liu, L.-F. Wang and M.-L. Tong, *Chem. Commun.*, 2015, **51**, 10291-10294.
106. P. Gnutek and C. Rudowicz, *Opt. Mater.*, 2008, **31**, 391-400.
107. P. Dorenbos, *J. Phys.: Condens. Matter*, 2003, **15**, 575.
108. B. G. Wybourne, *Spectroscopic Properties of Rare Earths*, Interscience, New York, 1965.
109. C. A. Morrison, *Angular Momentum Theory Applied to Interactions in Solids*, Springer, Berlin, 1988.
110. C. Görller-Walrand and K. Binnemans, in *Handbook on the Physics and Chemistry of Rare-Earths*, eds. K. A. J. Gschneidner and L. R. Eyring, Elsevier, Amsterdam, 1996, vol. 23, ch. 155.
111. J. Mulak and Z. Gajek, *The Effective Crystal Field Potential*, Elsevier, Amsterdam, 2000.

112. W. T. Carnall, H. Crosswhite, H. M. Crosswhite, J. P. Hessler, N. Edelstein, J. G. Conway, G. V. Shalimoff and R. Sarup, *J. Chem. Phys.*, 1980, **72**, 5089-5102.
113. C. Rudowicz, *Magn. Reson. Rev.* , 1987, **13**, 1.
114. C. Rudowicz, *Erratum, ibidem*, 1988, **13**, 335.
115. C. Rudowicz and Karbowiak M., *Coord. Chem. Rev.*, 2015, **287**, 28.
116. C. Rudowicz and J. Qin, *J. lumin.*, 2004, **110**, 39.
117. C. Rudowicz and P. Gnutek, *Physica B*, 2010, **405**, 113.
118. C. Rudowicz, *Chem. Phys.*, 1985, **97**, 43.
119. C. Rudowicz, *J. Chem. Phys.*, 1986, **84**, 5045.
120. C. Rudowicz, M. Chua and M. F. Reid, *Physica B*, 2000, **291**, 327.
121. C. Rudowicz, P. Gnutek and M. Karbowiak, *Opt. Mater.*, 2011, **33**, 1557.
122. D. J. Newman and B. Ng, *Rep. Prog. Phys.* , 1989, **52**, 99.
123. D. J. Newman and B. Ng, eds. D. J. Newman and B. Ng, University Press, Cambridge, 2000, ch.5.
124. M. Andrut, M. Wildner and R. C., in *Spectroscopic Methods in Mineralogy – EMU Notes in Mineralogy*, eds. B. A. and L. E., Eötvös University Press, Budapest, 2004, vol. 6, ch. 4, p. 145.